
Structure of Convective Storms

TETSUYA FUJITA

University of Chicago, Chicago, Illinois

Reprinted from MONOGRAPH NO. 5, AMERICAN GEOPHYSICAL UNION, 1960
Physics of Precipitation
Printed in U.S.A.

Structure of Convective Storms

TETSUYA FUJITA

University of Chicago, Chicago, Illinois

Abstract—The features of the Fargo tornadoes and the meteorological situations producing them are studied in three scales: macroscale, dealing with the precipitation and tornado distribution over three-fourths of the United States; mesoscale analysis of North and South Dakota and of the rotating cloud which produced four tornadoes as it moved over the Fargo area; and, finally, microscale features of the tornado itself. These analyses are presented in an animated 16 mm motion picture. Included in this report are the results of the computed cyclostrophic wind speed and rotational speed of the funnel of the Fargo tornado. A proposed mechanism of an irreversible process taking place inside the inflowing air toward the tornado funnel is also presented.

Life cycle of the Fargo tornado—By using the still photographs and movie films collected through WDAY-TV, Fargo, and the U. S. Weather Bureau at Hector Airport, Fargo, changes in the tornado funnel throughout its life span were obtained. Figure 1 reveals that the funnel dropped from the cloud base to the ground within a matter of minutes. As soon as the tip of the funnel reached the surface, the lower portion of the funnel was sheared off, and then rounded; meanwhile, the funnel diameter above the rounded bottom kept increasing. Soon after, the tornado funnel as a whole started shrinking at about 18h 30m CST.

The diameter of the funnel is also given in Figure 1 as a function of time and the height above the surface.

Funnel diameter and centrifugal acceleration—An expanded analysis of the funnel diameter is made for the period of only 2½ minutes during which the tornado funnel reached the ground and was rounded at its bottom. The rounded funnel bottom shows an extremely high rate of increase in diameter along the vertical (Fig. 2).

Assuming that the condensation is taking place at the funnel edge and that the condensation pressure is the same everywhere at the smooth edge of the funnel, the hydrostatic assumption and the cyclostrophic wind equation enable us to describe

$$-\frac{1}{\rho} \frac{\Delta P}{\Delta R} = \frac{V^2}{R}$$

$$\Delta P = -\rho g \Delta Z$$

Therefore, we have

$$\frac{\Delta Z}{\Delta R} = \frac{V^2}{R} \bigg/ g$$

where V is the cyclostrophic wind speed; ρ , the density; R , the radius; P , the pressure. This equation shows that the tangent of the funnel slope is proportional to the centrifugal acceleration in the unit of gravitational acceleration. It is of interest to see the maximum centrifugal acceleration 10.8 g occurring at about 18h 28.8m at 120 m above the ground (Fig. 3).

Cyclostrophic wind speed—The cyclostrophic wind speed computed from the centrifugal acceleration is shown in Figure 4 as a function of time and the height above the ground. The diameter of the funnel is also indicated by broken lines. The computed wind speed is the cyclostrophic wind speed at the funnel edge. No speed was computed at the bottom of the rounded funnel because its gradient is so small that it would give less than 10 m/sec, while heavy damage was taking place directly beneath the funnel.

In any case, the tangential speed at the edge of the funnel above the rounded bottom gives a fairly high value, which would be expected from the tornado damage. The maximum speed of 103 m/sec, or 230 mph, occurred slightly before 18h 29m when the funnel diameter, 130 m above the ground, was 200 m.

A film taken by WDAY-TV, Fargo, at the time of the Fargo tornado permits us to make an independent computation of the rotation speed of the funnel. Figure 5 indicates the tangential speeds computed by cyclostrophic assumption (double lines) and tornado film (heavy lines) for three different times: 18h 28.0m, 18h 28.9m, and 18h 29.6m CST. The computation is made along the dotted line, along the funnels shown at the top of the figure. At the present time, so far as the Fargo

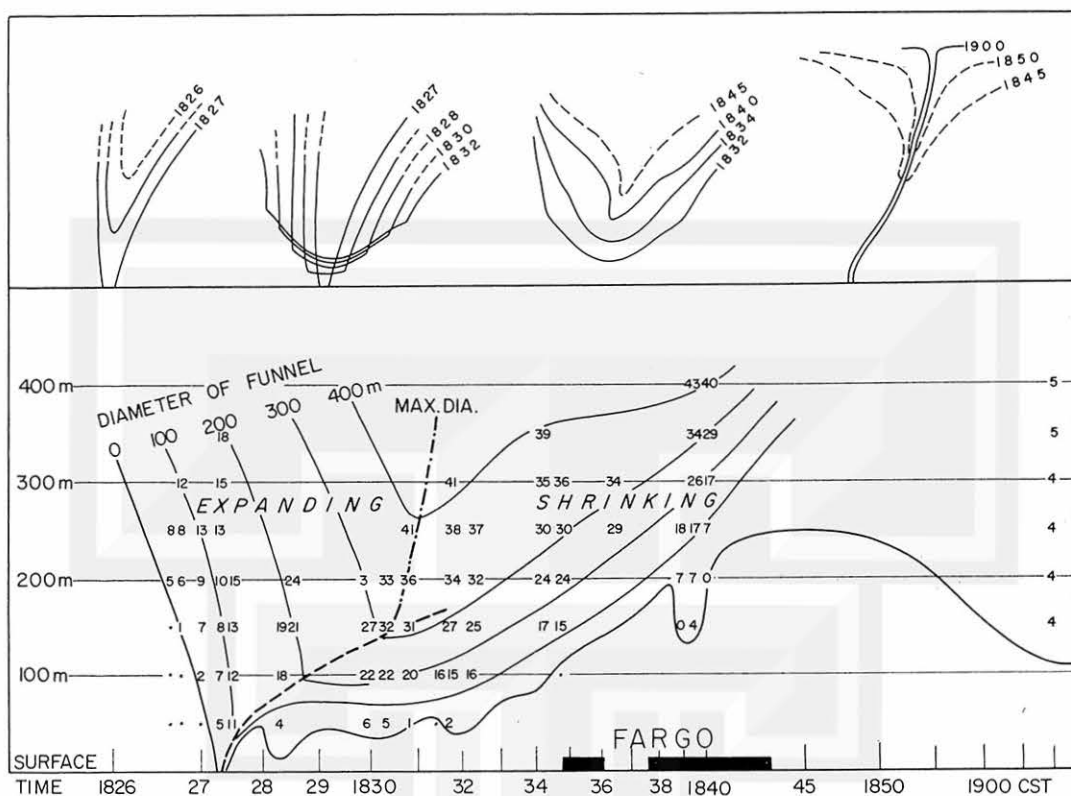


FIG. 1—Life cycle of the Fargo Tornado of June 20, 1957, determined by using about 200 photographs taken by Fargo-Moorhead citizens during the time of the storm; the cone-shaped funnel reached the ground only a minute after its appearance at the base of the tornado-producing cloud; the entire life of the storm was about 30 minutes

tornado is concerned, no way of computing wind speed inside or outside the funnel has been found.

Tangential wind speed at the funnel edge is summarized in Figure 6 as a function of time and the radius of the funnel. The dashed line in the figure denotes the radius of the rounded portion of the funnel which appeared at 18h 28m CST, then increased rapidly in diameter.

The slope of the rounded bottom funnel, which would have maintained the cyclostrophic wind speed obtained by using the movie taken by WDAY-TV, should be at least five times steeper than it actually was. At one time the rounded bottom of the funnel was almost flat, yet it was rotating at over 100 mph. This suggested that the constant pressure surface should cut through the bottom of the funnel.

Irreversible process taking place inside tornado inflow—The previous discussion indicates that the constant pressure surfaces maintaining the high-speed cyclostrophic wind at the base of the rounded bottom funnel must have been much steeper than the funnel itself.

A schematic figure of constant pressure surfaces in relation to a rounded bottom funnel is shown in Figure 7. We should reconsider the thermodynamical process taking place inside the air flowing into the tornado funnel.

The dry adiabatic process in the parcel method is an adiabatic reversible process in thermodynamics. No heat should be added or produced along the course of the expansion of a parcel. This would result in the same condensation pressure regardless of the path of the parcel so long as it starts expanding under the same initial conditions.

Through an irreversible adiabatic process, however, heat is continuously produced internally while the parcel expands. Parcel A₄, for instance, will show a small rate of cooling when it flows into a tornado, because the parcel moves near the ground under the influence of frictional force which produces heat; meanwhile the parcel loses its mechanical energy. Thermodynamically, the line along which the parcel expands lies between isentrope and isenthalpe on adiabatic charts.

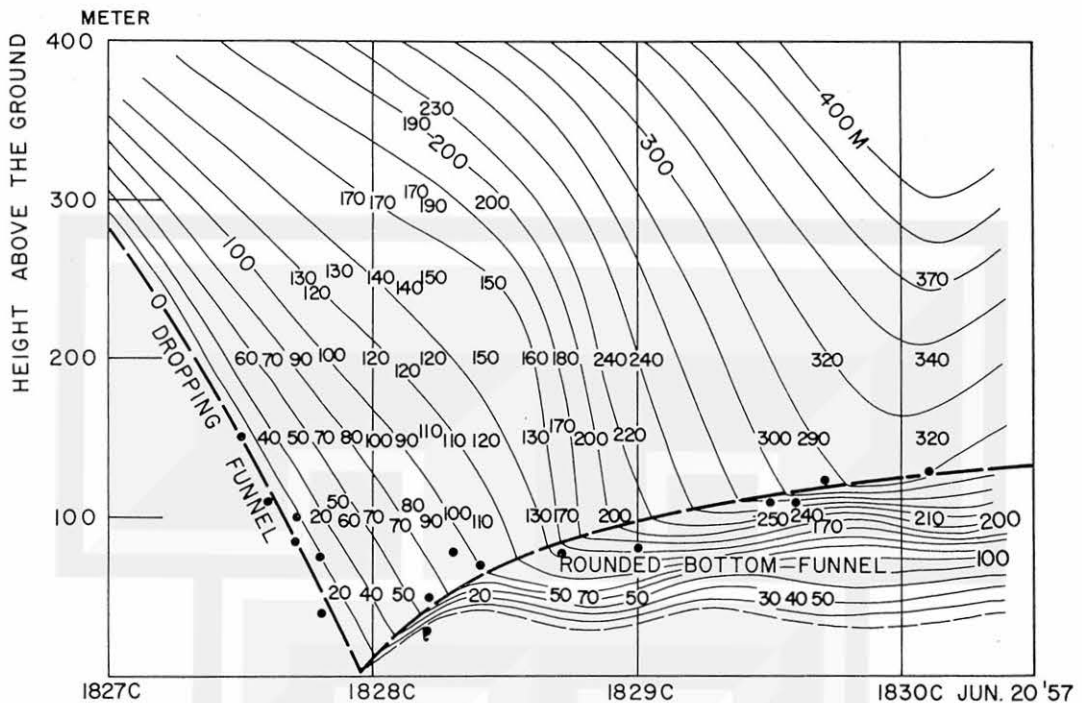


FIG. 2—Detailed description of the cone-shaped funnel in its early stage; the bottom of the funnel was rounded, and lifted upon reaching the ground; isopleths are funnel diameters in meters

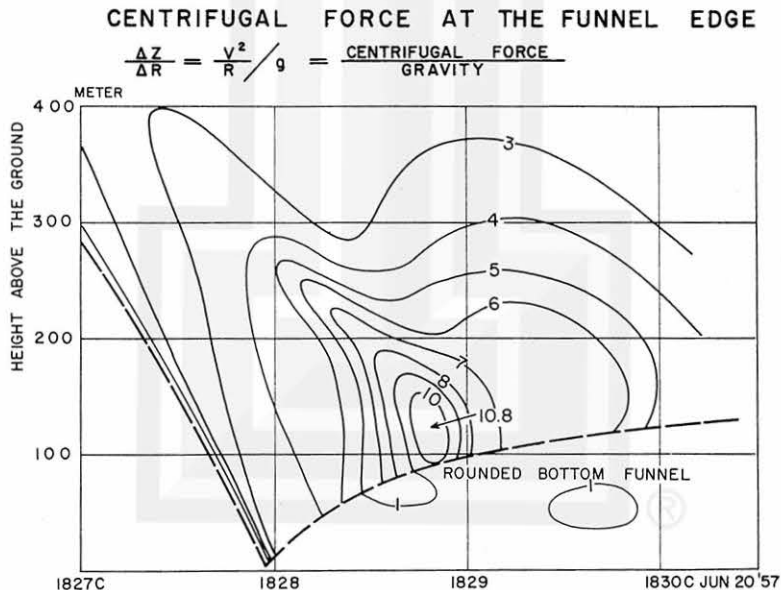


FIG. 3—Vertical and time change in centrifugal force acting upon the parcel circling around the funnel; wind is assumed to be cyclostrophic

Now, the illustration shows that the parcels expanding along stream lines $A_0-A_1-C_1$ and $A_0-A_2-C_2$ are friction free; therefore, the moisture inside the parcel would condense at C_1 and C_2 lo-

cated at the surface of the same condensation pressure. On the other hand, the parcels following the paths $A_0-A_3-C_3$ and $A_0-A_4-C_4$ would increase their entropy through their irreversible expan-

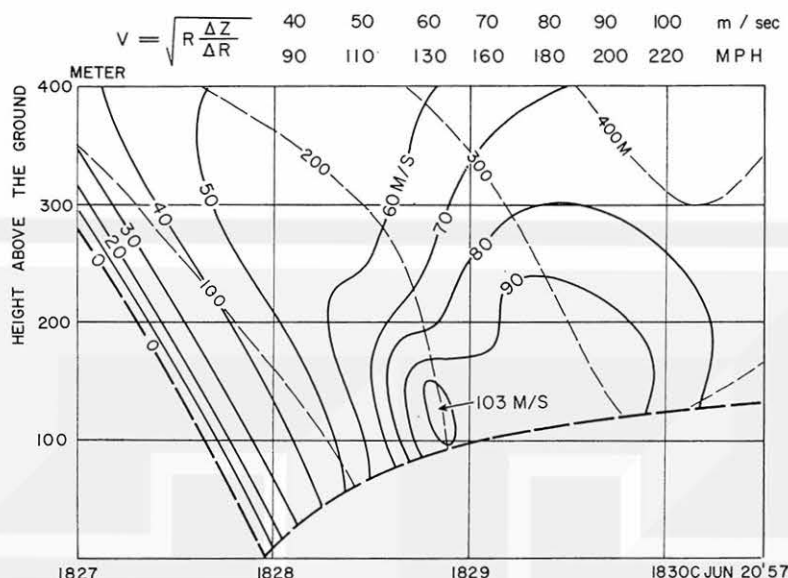


FIG. 4—Cyclostrophic wind speed computed from the gradient of the edge of the funnel; the maximum speed, 230 mi/hr, appeared shortly before 18h29m CST at the 100-meter level; no computation was made for the portion of the rounded bottom where the wind was far from being cyclostrophic

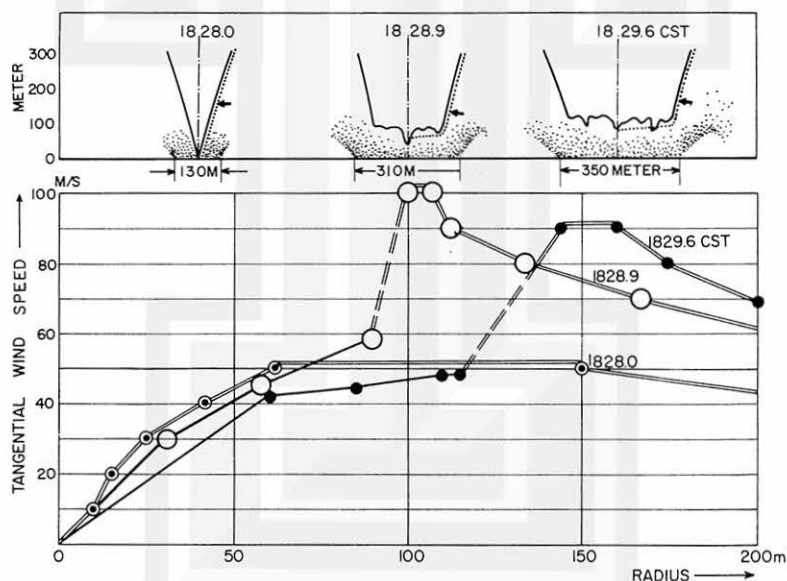


FIG. 5—Radial distribution of tangential wind speed in meters per second; arrows in upper figures give the location of the maximum wind speed computed along the dotted lines

sion, reaching their condensation pressures at C_3 and C_4 , respectively. Assuming that the expansion along the surface is given by a straight line $A_0-A_3'-A_4'$ on the adiabatic diagram, and that the expansion along A_3-C_3 and A_4-C_4 is dry adiabatic and reversible, the temperature and pressure

change of parcels flowing into the bottom of the rounded bottom funnel were qualitatively described.

Conclusions—It was found that the cyclostrophic wind speed computed from the shape of the funnel with the combined use of hydrostatic

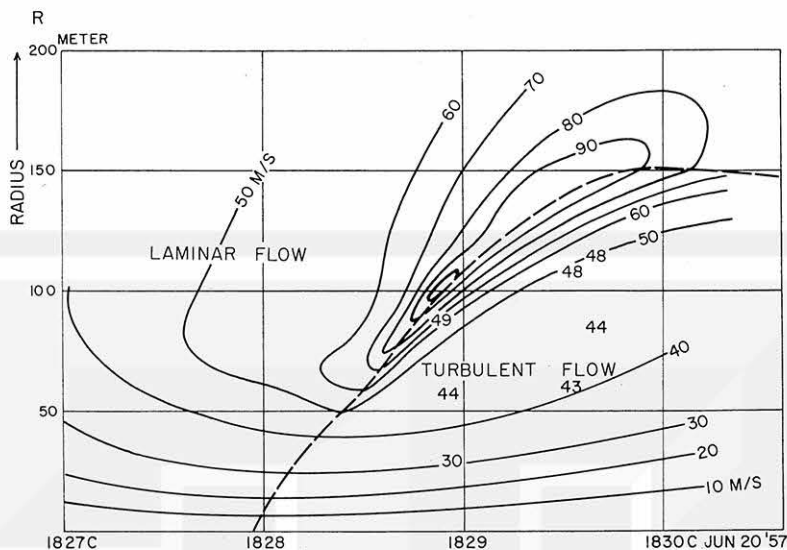


FIG. 6—Tangential wind speed shown as a function of time and radius of the funnel; the dashed line indicates the radius of the rounded bottom funnel

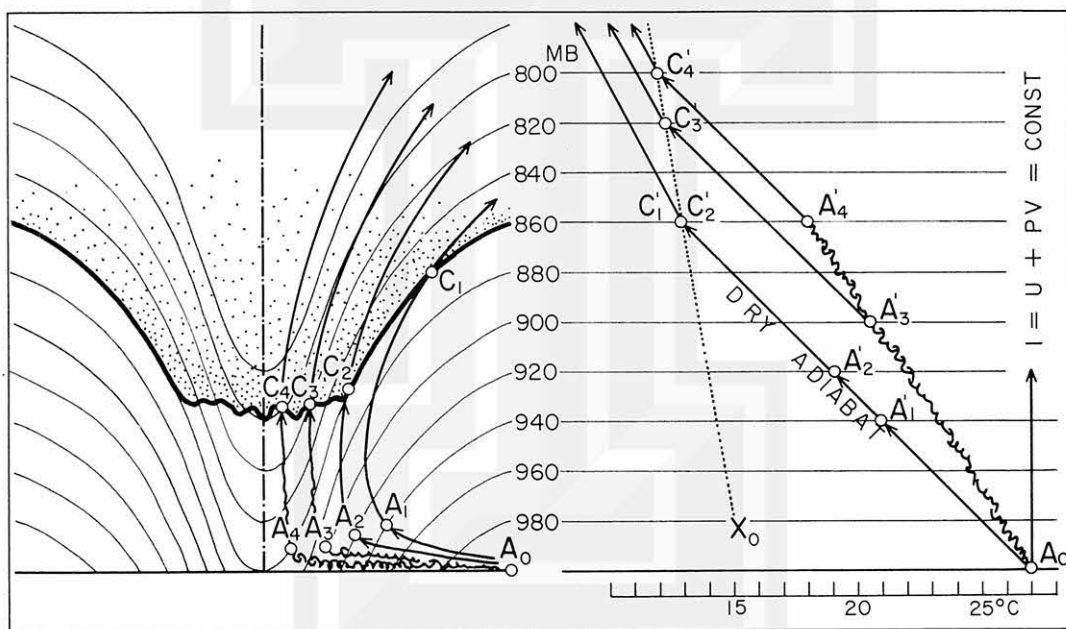


FIG. 7—The nonadiabatic process taking place beneath a tornado funnel after it is rounded; note that the edge of the rounded funnel no longer represents a surface of condensation pressure

and condensation pressure in the parcel method shows reasonable values. However, as soon as the funnel reaches a certain diameter, large enough to provide a long spiral inflow path of the parcels near the ground, the lower portion of the funnel is rounded. At this stage the bottom of the funnel no longer maintains the same condensation pres-

sure. A dry adiabatic irreversible process associated with the near ground inflow was found to be one of the explanations for this.

Acknowledgment—The research reported in this paper has been sponsored by the U. S. Weather Bureau under Contract Cwb 9530.

Editor's Note—After having presented his lecture Dr. Fujita showed an animated cinema of the Fargo Tornado on June 20, 1957. The film is divided into three parts: (1) the synoptic pattern

with isobars and moving precipitation systems, (2) the meso-scale analysis of the Tornado proper, and (3) micro-scale features of the funnel and the movement of clouds near and around it.

Discussion

Dr. Malkus—I am sure we would all like to congratulate Dr. Fujita for a fascinating physical study of tornadoes in this marvelous animated

film which illustrates it. Only those of us who tried to make films ourselves realize the enormous amount of effort that goes into it.

